Int. J. Electrochem. Sci., 15 **(2020)** 4032 – 4055, doi: 10.20964/2020.05.57

International Journal of
ELECTROCHEMICAL
SCIENCE
www.electrochemsci.org

Inhibition Corrosion Effect of Extract from Basella rubra on Carbon Steel in HCl Solution

Cuijie Shi[1,2], *XiaoPing Song*[1], *Ying Kan*[1], *Yu Fan*[2,*], *Xiaowei Song*[1], *Yinglan Zhang*[3,4], *Zhengdong Zhang*[1,*]

[1] National Institute of Metrology, Beijing 100029, China
[2] College of Chemical Engineering and Environment, China University of Petroleum—Beijing, Beijing 102249, China
[3] Leibniz-Institut für Polymerforschung Dresden, Germany
[4] Technische Universität Dresden, Germany
[*]E-mail: zhangzhengdong@nim.ac.cn (Z. Zhang); fanyu@cup.edu.cn (Yu Fan)

Received: 9 January 2020 / *Accepted:* 17 february 2020 / *Published:* 10 April 2020

The inhibition behavior of fruit extract of *Basella rubra* on corrosion of carbon steel in 1 mol L^{-1} HCl solution was studied by weight loss and electrochemical methods. The adsorption of extract obeys Langmuir adsorption isotherm. Electrochemical results reveal that the inhibitor acts as mix type inhibitor but cathodically predominant. The separated substituents can also inhibit the corrosion of carbon steel in HCl solution efficiently. SEM and XPS results demonstrate that the protective layer formed by extract molecules can effectively inhibit corrosion process at metal surface.

Keywords: Carbon steel; Corrosion inhibitor; Weight loss; EIS; HCl solution

1. INTRODUCTION

Metals and alloys are intensively suffered from corrosion attack in industrial applications, particularly in acid media, which is universally existed in the industry. The major applications are acid pickling, oil and natural gas exploitation, transportation and refinery of crude oil, recirculating cooling water system, oil-well acidizing, etc. [1–4]. As one of the effective methods to reduce the dissolution of metals and consumption of acid, the addition of corrosion inhibitor in acid media is universally applied in the industry. A great many of corrosion inhibitors were applied in industry to solve this problem. These inhibitors are mainly including organic and inorganic corrosion inhibitors [5]. Organic corrosion inhibitor, most widely used one in recent applications, is often consisted of organic groups containing N, O, S, P atoms or π bonds [6–8]. Most of the inorganic inhibitors, like dichromate, nitrite, arsenide and so on, have serious environmental problems. Scientists are eager to find corrosion inhibitors, which

are environmental friendly, to replace the present inorganic and organic corrosion inhibitors. Hence, inhibitors from natural plants become more and more popular. Extracts from different natural plants have been exploited as corrosion inhibitors in recent years. Some of these inhibitors are not only friendly to environment, but also inexpensive, readily available, renewable and degradable [3].

A lot of extracts from natural plants, such as leaves, flowers, fruit peels and fruits of plant, have been exploited as corrosion inhibitors. Quraishi applied the *Murraya koenigii* leaves extract as corrosion inhibitor for mild steel in hydrochloric acid and sulfuric acid solutions. The results showed that the extract acted as excellent inhibitor for mild steel in both solutions [9]. Abd-El-Khalek investigated the corrosion inhibition of *Nicotiana* leaves extract as corrosion inhibitor for steel in acidic and neutral solutions. Results revealed that this extract acted as mix type corrosion inhibitor for steel in acidic solution and anodic type corrosion inhibitor in neutral solution. They also found that the inhibitive performance of *Nicotiana* leaves extract in acidic medium behaved better than in neutral medium [10]. Olusegun Sunday studied the inhibition behavior of *Jatropha Curcas* leaves extract for mild steel in HCl solution. Results manifested that it can effectively inhibited the corrosion of mild steel in HCl solution. The adsorption of inhibitor accorded the Langmuir isotherm. It was also found that the inhibitor adsorbed on metal surface via chemisorptions [11]. Punita Mourya utilized the *Tagetes erecta* (*Marigold flower*) extract as corrosion inhibitor for mild steel in acid solution. The polarization curves proved the extract acted as mix type corrosion inhibitor. Langmuir adsorption isotherm fits the best. The activation parameters revealed that the extract was physically adsorbed on metal surface [12]. Ostovari investigated the corrosion inhibition of henna extract and its constituents for mild steel in HCl solution. They found that all tested compounds acted as mixed inhibitor. The inhibition efficiency reached 92.06% in the presence of 1.2 g L^{-1} henna extract [13]. Odewunmi used the *Watermelon rind* extract as green inhibitor for mild steel in acid medium. Polarization curves results revealed this extract acted as mix-type inhibitor, adsorption of this extract obeyed Temkin adsorption isotherm [14]. Nouha researched on the inhibition behavior of *Orange peel* extract and its main antioxidant compounds for carbon steel in acidic medium. They found that all compounds inhibit the corrosion of steel through both adsorption and precipitation on steel surface [15]. Tecnologia applied the aqueous extract of *Mango* as corrosion inhibitor for carbon steel in HCl solution. Inhibition of 97% was reached in the presence of 400 mg L^{-1} *mango* extract after immersing 24h. The adsorption of extract components obeyed Langmuir adsorption isotherm [16]. N. El investigated *Retama monosperma (L .) Boiss.* seeds extract as eco-friendly inhibitor for metal in HCl solution. The results showed that the extract acted as effective corrosion inhibitor in HCl medium. High inhibition efficiency (94.4%) was obtained in the presence of 400 mg L^{-1} extract at 303 K [17]. El-Etre studied the inhibition of *Khillah* extract for SX 316 steel in acid solution. Results revealed that the extract remarkably decreased the corrosion rate of steel in acid solution [18]. These extracts exhibit excellent inhibitive performance, which is owing to in the presence of natural compounds to form a protective layer on metal surface, thus to alleviate corrosion.

Basella rubra, a widely distributed plant in subtropical zone of Asia, is used as food and herb medicine since ancient China. The leaf of *Basella rubra* is commonly used as vegetable food on the dinning-table of many Chinese. Previous study showed that the leaf extract of *Basella rubra* is excellent corrosion inhibitor for mild steel in 1 M HCl solution [19]. Additionally, the fruit of *Basella rubra* has been used as natural dyestuff for a long history. The fruit exhibits a red purple appearance. The colorful

compound can be adsorbed on solid surface easily and hardly be washed off, indicating excellent adsorption ability which might be useful as corrosion inhibitor. It is believed that betanin, isobetanin and gomphrenin I are the major pigment ingredients in *Basella rubra*. The structures of these compounds are shown in Fig. 1 [20,21]. The structure of main pigment ingredients in *Basella rubra* includes O, N atoms and π bonds, which is in accordance with the structure of usual corrosion inhibitor. Therefore, the compounds are promising to become excellent natural corrosion inhibitor.

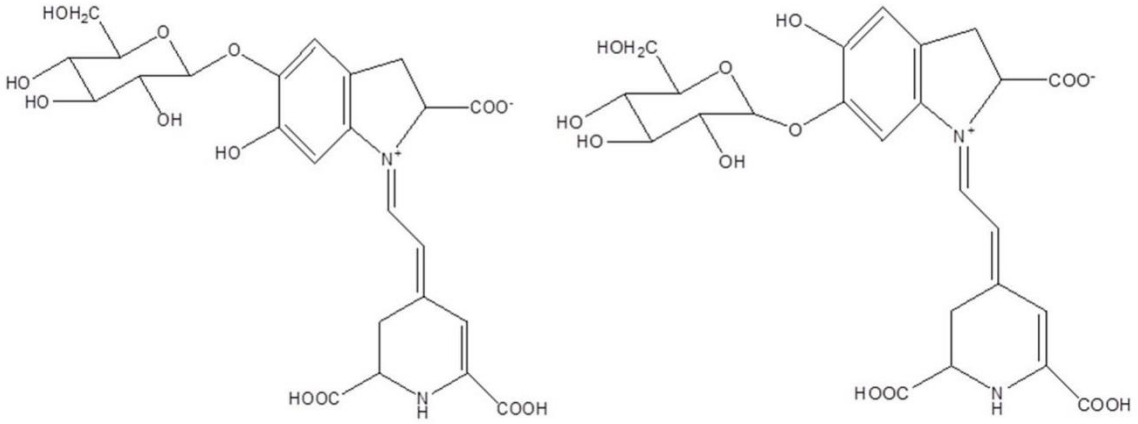

Figure 1. Structures of betanin and gomphrenin I

In this paper, the fruit extract of *Bsaella rubra* was applied as environmental friendly corrosion inhibitor for carbon steel in 1 M HCl solution via weight loss, electrochemical experiments and scanning electron microscopy. Influences of temperature, concentration and immersion time on corrosion rate and inhibition efficiency were discussed. Furthermore, the inhibition properties of substituents of the extract were compared in detail. Finally, the adsorption behavior and inhibition mechanism were also discussed.

2. EXPERIMENTAL DETAILS

2.1 Preparation of natural corrosion inhibitor

Basella rubra fruit was washed by deionized water to remove mud and dust, dried in electric thermostatic drying oven at 333 K and smashed by a comminuting machine to obtain the powder. 10 grams of powder was added into 50 mL HCl (1 mol L^{-1}) with stirring at room temperature for 5 h. The mixture was filtered to acquire the solution, and dried the residue in an oven at 333 K for one day. The residue was weighed to affirm the concentration of extract. The mixture solution was preserved in a refrigerator.

The constituents (C1, C2 and C3) were obtained by crude extract from mixture solution. 100 ml of mixture solution was condensed to 20 ml. Then 80ml of anhydrous ethanol was added to the condensed mixture solution. Next step was centrifuging with 4000 r/min for 20 min to separate the precipitate and solution. Then the precipitate was washed by 95% ethanol three times, filtrated and dried

to obtain compound 1 (C1). The solution continued to be condensed to 1/5 of the initial volume of the filtrated solution. The pH value of the new solution was adjusted to above 12 by adding potassium hydroxide solution. After further centrifuging and repetitive washing, precipitate (compound 2, C2) and solution were obtained separately. 1 mol L^{-1} HCl was added to the new solution to adjust the pH value to 7. After further condensation, anhydrous ethanol was added to the solution to separate out KCl crystal. The solution was dried to obtain compound 3 (C3). All the three constituents were further dried in an oven at 333 K for one day before use.

2.2 Weight loss measurement

Three parallel carbon steel sheets of 40 mm×13 mm×2 mm were abraded with different emery papers (grade 180, 320, 500, and 1000) gradually, washed with deionized water, acetone, anhydrous ethanol, and then dried with a cold drier. After weighing by electronic analytical balance with sensitivity of ±0.1 mg, the samples were suspended in solutions of 500 mL 1 mol L^{-1} HCl solution at different temperatures (293, 313, 333 and 353 K), controlled by water thermostat. After 4 hours' immersion, the samples were taken out, carefully removed the corrosion products, washed, dried with a cold drier and re-weighed accurately. The weight loss was obtained for every sample and used the following equation (Eq. (1)) to calculate the corrosion rate.

$$CR = \frac{\Delta m}{St} \quad (1)$$

where $\triangle m$ is the weight loss of carbon steel, S represents the total area of one carbon steel sample, t is immersion time (4 h). In order to obtain more reliable results, the corrosion rate was the mean value of three parallel carbon steel sheets. The inhibition efficiency (η) was calculated by follow equation (Eq. (2)):

$$\eta = \frac{CR_0 - CR_1}{CR_0} \times 100\% \quad (2)$$

where CR_0 and CR_1 stand for corrosion rate of carbon steel samples without and with extract, respectively.

2.3 Electrochemical measurements

Electrochemical experiments were carried out by the traditional three-electrode system, including a saturated calomel electrode as reference electrode, a platinum electrode as counter electrode and a working electrode. Working electrode was abraded as described above. Then the carbon steel sheet was connected with wire, sealed with epoxy resin leaving the exposed surface area of 1 cm^2 in solution.

All electrochemical experiments were carried out on a *Corr Test* electrochemical workstation (Wuhan Corrtest Instruments Corp., LTD CS350). Before the electrochemical impedance spectra (EIS) and potentiodynamic polarization curve (PC) measurements, the open circuit potential (OCP) was measured for 1 h until the potential was reached relatively stable. The EIS was measured in the frequency range of 100 kHz-0.01 Hz at stable OCP with 10 mV AC amplitude. Potentiodynamic polarization curves were recorded from -300 mV to +300 mV (vs. OCP) at scan rate of 0.5 mV s^{-1}. The inhibition efficiency (η) was calculated from EIS and PC as follow relations (Eqs. (3) and (4)), respectively.

$$\eta = \frac{R_{ct}^{'}-R_{ct}^{0}}{R_{ct}^{'}} \times 100\% \quad (3)$$

$$\eta = \frac{I_{corr}^{0}-I_{corr}^{'}}{I_{corr}^{0}} \times 100\% \quad (4)$$

where R_{ct}^{0} and I_{corr}^{0} represent charge transfer resistance and corrosion current density in the absence of extract, $R_{ct}^{'}$ and $I_{corr}^{'}$ stand for charge transfer resistance and corrosion current density in the presence of extract. All experiments in different conditions were tested at least two or three times to ensure the good reproducibility.

2.4 Scanning Electron Microscopy (SEM)

The carbon steel sheets of 40 mm×13 mm×2 mm were immersed in 1 mol L^{-1} HCl solution without and with 1 g L^{-1} extracts at 293 K for 4 hours, washed by deionized water, dried with a cold drier and then tested by SEM (EVO MA15, ZEISS).

2.5 Fourier transform infrared spectrophotometer (FT-IR) and X-ray photonic spectroscopy (XPS)

The extracts and the separated constituents from extract were characterized by FT-IR. KBr disk technique was used to prepare samples and then the samples were tested in FT-IR (Nicolet Instrument Corporation, Madison, WI). The range of wavelength was from 4000 cm^{-1} to 400 cm^{-1}.

In XPS measurements, carbon steel sheets of 4 mm×4 mm×2 mm were abraded with different emery papers (grade 180, 320, 500, 1000, and 2000), washed with deionized water, acetone, ethanol, and then dried with a cold drier. The steel samples were immersed in 1 mol L^{-1} HCl solution with 1g L^{-1} C1, C2, C3 and extracts at 293 K for 4 hours. After 4 hours' immersion, samples were removed and washed by deionized water and ethanol, then dried with a cold drier. All samples were tested in ESCALAB 250 spectrometer (ThermoFisher Scientific USA) with the monochromatized Al-Kα X-ray source (150 W). The analyzer was operated in constant pass energy of 200 eV for survey and 30 eV for high resolution scans, used the large area XL lens mode. The experimental data were analyzed by XPS PEAK 41 software.

3. RESULTS AND DISCUSSION

3.1 Corrosion inhibition behavior from weight loss measurement.

Fig.2 shows the influence of temperature and inhibitor concentration on corrosion rate and inhibition efficiency of *Basella rubra* fruit extract on carbon steel in 1 M HCl solution. It is shown that the corrosion rate rapidly decreases with the increase of inhibitor concentration and inhibition efficiency rises quickly correspondingly, which indicates that the inhibitor is very effective in 1M HCl solution. By comparing the inhibition efficiency between inhibitor concentration of 0.10 g L^{-1} and 1.00 g L^{-1}, it is found that inhibition efficiency increases slowly, which can be attributed to saturation of surface coverage by inhibitor molecules adsorbed on the metal surface [1,22]. It is also shown that in

concentrations higher than 0.50 g L^{-1}, the inhibition efficiencies in all temperatures are higher than 80%. Maximum inhibition efficiency of 94.8% occurs at extract concentration of 1.00 g L^{-1} at 293 K.

The temperature also has remarkable impact on corrosion rate and inhibition efficiency. The inhibitor exhibits excellent inhibition performance in all measured temperatures. The inhibition efficiency varies slightly at temperatures below 313 K in the same concentration of extract, which is quite different from temperatures above 313 K. The corrosion rate drastically increases and inhibition efficiency declines sharply at 353 K. Although it is also very effective, the inhibition performance weakens at higher temperature. It can be ascribed to desorption of inhibitor molecules at high temperature or degradation of inhibitor molecules [23,24].

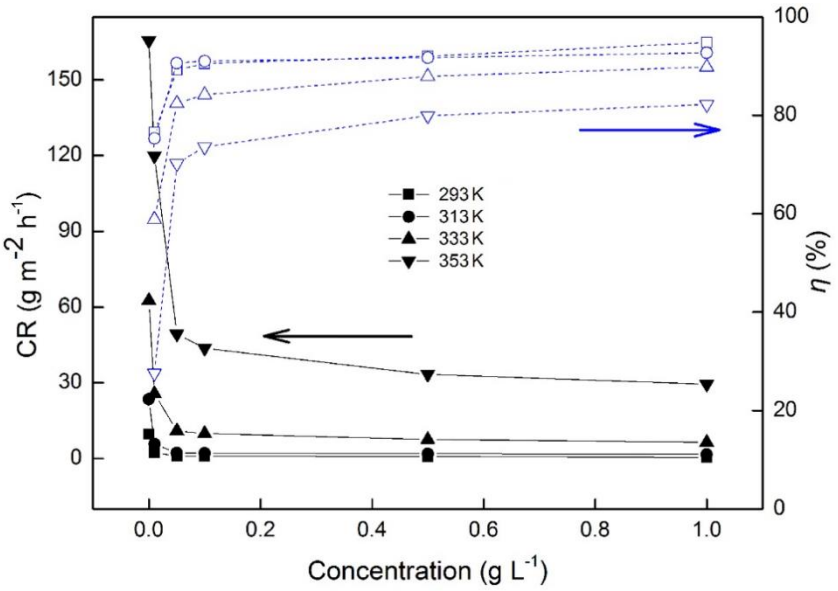

Figure 2. Corrosion rate and inhibition efficiency (η) varied with concentration and temperature from weight loss experiments of carbon steel in 1 M HCl in the absence and presence of different concentrations of Basella rubra extract at 293-353 K.

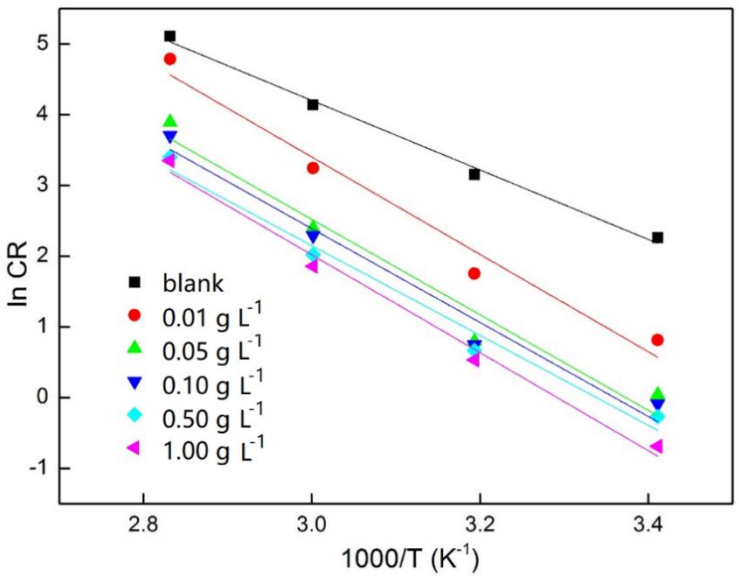

Figure 3. Arrhenius plots for the corrosion rate of carbon steel in 1 M HCl with different concentrations of extract

For better understanding the effect of temperature on corrosion reaction process, the Arrhenius equation was used to calculate the relative parameters of the corrosion process [25]:

$$CR=A\,exp(-\frac{E_a}{RT}) \quad (5)$$

where CR, E_a, R, T and A represent the corrosion rate, activation energy, gas constant, absolute temperature and pre-exponential factor, respectively.

Table 1. Thermodynamic parameters for the corrosion of carbon steel in 1 M HCl with various concentrations of extract

C (g L^{-1})	E_a (kJ/mol)	$\triangle H_a$ (kJ/mol)	$\triangle S_a$ (J/mol K)
Blank	41	38	-96
0.01	57	55	-54
0.05	56	54	-64
0.10	55	53	-68
0.50	53	50	-77
1.00	58	55	-64

The plot of ln CR versus 1000/T is shown in Fig. 3 from the data of Fig. 2. Activation energy (E_a) was calculated by the slope of the straight line of ln CR versus 1000/T. The value of activation energy is listed in Table 1. The apparent activation energy with different concentration of inhibitor is higher than that in blank solution. It is suggested that the adsorption process is physisorption in nature if the E_a shifts positively with the presence of corrosion inhibitor. Otherwise, negative shifting stands for chemisorption in nature [26]. The value of E_a is 41 kJ/mol in blank solution and lower than E_a in the presence of extract, indicated that the extract adsorbed on the metal surface by physical adsorption. It is usually conveyed by formation of adsorption film via physical electrostatic [8].

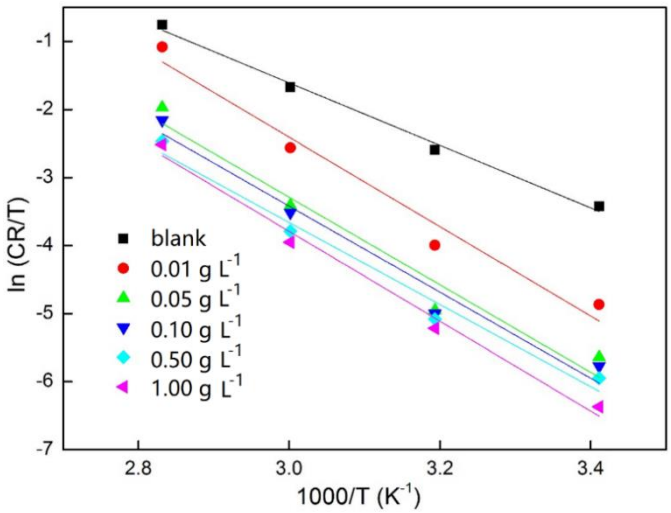

Figure 4. Plots of ln (CR/T) vs 1000/T for carbon steel in 1 M HCl with different concentrations of extract

Besides, the enthalpy of activation ($\triangle H_a$) and the entropy of activation ($\triangle S_a$) were obtained by alternative formulation of Arrhenius equation (Eq. (6)) [27]:

$$CR=\frac{RT}{Nh}exp(\frac{\Delta H_a}{R})\ exp(-\frac{\Delta S_a}{RT}) \quad (6)$$

where N is the Avogadro's constant, h is the Plank's constant. The relation between ln (CR/T) and 1000/T is depicted in Fig. 4. The values of enthalpy of activation ($\triangle H_a$) and the entropy of activation ($\triangle S_a$) are shown in Table 1. It is found that the values of $\triangle H_a$ in solutions with corrosion inhibitors are higher than that in blank solution. The positive value of $\triangle H_a$ indicates that the process of dissolution for carbon steel in acid solution is an endothermic process and this process slows down in the presence of extract. Both E_a and $\triangle H_a$ present the same tendency [8]. Compared with blank solution, it is noticeable that the values of $\triangle S_a$ in the presence of extract increase positively, which indicates that the inhibitor molecules repel water molecules at the metal surface, resulting in more disordered corrosion system. The same findings have reported previously [28,29].

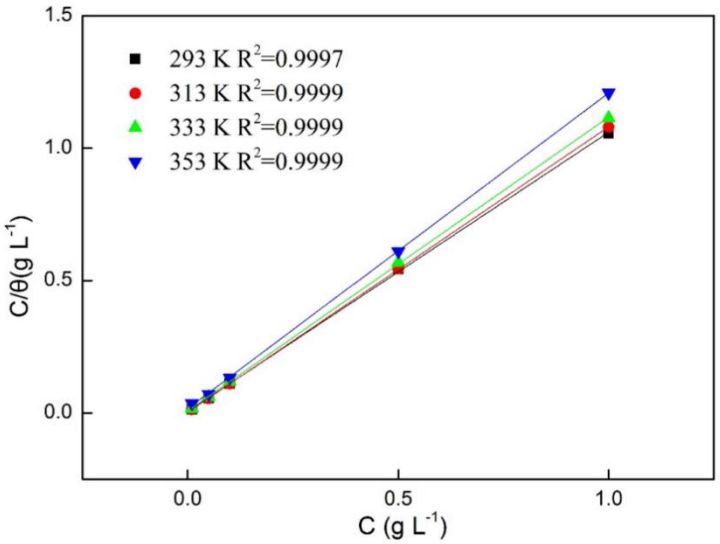

Figure 5. Langmuir adsorption plots for carbon steel in 1 M HCl with various concentrations of extract at different temperatures

Adsorption isotherm is useful to obtain more information about the adsorption mode of inhibitor on metal surface. It is commonly believed that the organic corrosion inhibitor adsorbs and covers on metal surface to retard corrosion process. The value of surface coverage (θ) is usually calculated by $\theta = \eta / 100$. In order to get the best adsorption mode, Langmuir, Frumkin, Freundlich and Temkin isotherms were applied to fit experiment results. It was found that Langmuir isotherm was the best mode of isotherm (shown in Fig. 5). Langmuir adsorption isotherm equation can be expressed as follows (Eq. (7) and (8)) [30,31]:

$$\frac{C}{\theta}=\frac{1}{K_{\text{ads}}}+C \quad (7)$$

$$K=\frac{1}{C_{\text{H2O}}}exp(-\frac{\Delta G^0_{\text{ads}}}{RT}) \quad (8)$$

where C_{H_2O} is the concentration of water. Fig. 5 demonstrates that the linear correlation coefficients (R^2) are very close to 1 at all temperatures, implying the adsorption of extract obeys the Langmuir adsorption isotherm accurately. The values of $\triangle G_{ads}{}^0$ at different temperatures are presented in Table 2. It is obviously that all values of $\triangle G_{ads}{}^0$ are negative in the range of temperatures, which imply

that the adsorption of inhibitor on carbon steel surface is a spontaneous process. In our present study, the values of $\triangle G_{ads}^{0}$ are with the range between -20 kJ mol^{-1} and -40 kJ mol^{-1} , which means that the adsorption of inhibitor belongs to mixed type adsorption(both physisorption and chemisorption) [31].

Table 2. The adsorption parameters derived from the Langmuir plots and values of $\triangle G_{ads}^{0}$ for carbon steel in 1 M HCl at different temperatures

T (K)	Slope	Intercept	$\triangle G_{ads}^{0}$ (kJ mol^{-1})
293	1.05	0.0071	-30
313	1.08	0.0027	-33
333	1.11	0.0083	-33
353	1.19	0.0121	-32

3.2 Electrochemical behavior of carbon steel in 1M HCl solution in the presence of inhibitor

3.2.1 Open circuit potential (OCP)

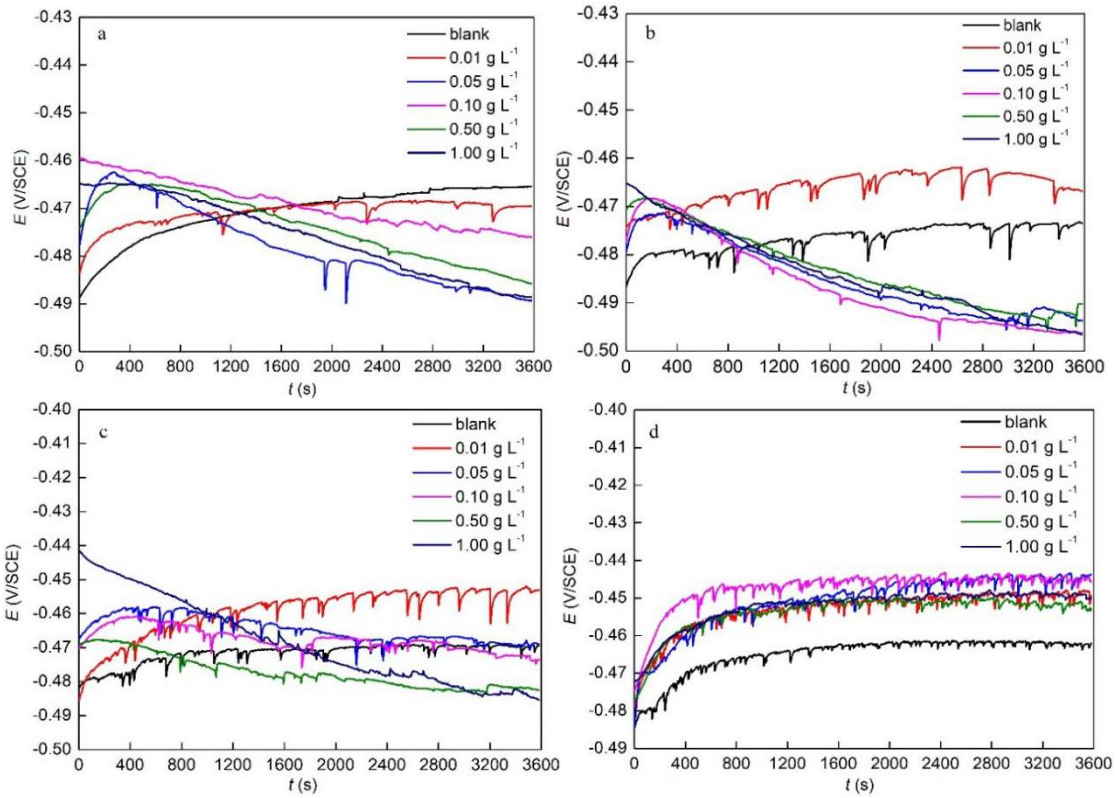

Figure 6. Open circuit potential (OCP) of carbon steel without and with different concentrations of extract in 1 M HCl at different temperatures: a) 293 K, b) 313 K, c) 333 K, d) 353K.

Fig. 6 shows the OCP of carbon steel with different concentrations of inhibitor in 1 M HCl at different temperatures. In Fig. 6 a, b, and c, OCP gradually moves positively during the period of immersion time, and the value gets stable after 2000 s in blank solution, which implies the OCP value has reached stable state. The OCP variations exhibit similar tendency in the presence of low concentrations of extracts. In the presence of high concentrations of inhibitor, OCP shifts towards

negative potential with the immersion time prolonged and the values reach stable state after 1 hours' immersion, which indicates that the inhibitor forms a protective inhibitor film on the electrode surface. Moreover, it is noticeable that the OCP value in inhibitor solution shifts to less positive and reaches maximum. Then the value decreases to reach the stable state. This tendency reveals that two opposite processes happened. One process is the forming of a protective layer by inhibitor molecules on the work electrode surface, which leads to inhibition of the corrosion process. Other process is corrosion, as a result of decreasing of the potential to negative direction [15,32–34]. Fig.6 (d) clearly demonstrates that the values of OCP reach stable state after 1200 s in the absence and presence of extract. The negative value of OCP in blank solution implies the breakdown of oxide film, which formed in the air before immersion on the electrode surface. Besides, the stable state potential of carbon steel shifts to less positive direction in the presence of extract solution. This behavior suggests that high resistance to the charge transfer happens on the carbon steel surface. The OCP shifting towards noble values in inhibitor solution implies a process, in which a protective layer forms on the metal surface and results in inhibiting the corrosion of steel in HCl solution [34,35].

3.2.2 Potentiodynamic polarization curves

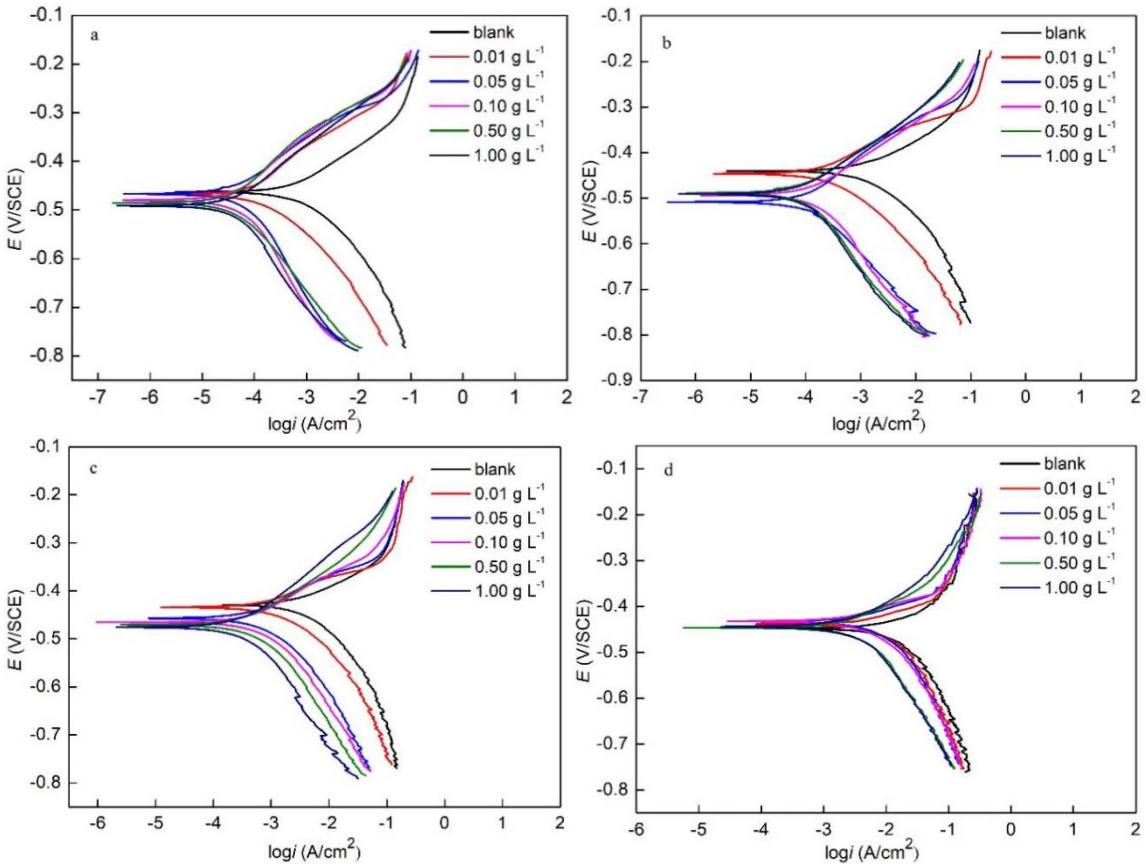

Figure 7. Polarization curves of carbon steel in 1 M HCl solution in the absence and presence of different concentrations of extract at different temperatures: a) 293, b) 313K, c) 333 K, d) 353 K.

Table 3. Parameters of polarization curves of carbon steel in 1 M HCl solution with different concentrations of extract at different temperatures

C (g L^{-1})	T (K)	E_{corr} (mV)	B_a (mV·dec^{-1})	-B_c (mV·dec^{-1})	I_{corr} (μA·cm^{-2})	η (%)
0		-463	83	98	647	-
0.01		-461	93	90	156	76
0.05	293	-467	108	160	65	90
0.01		-480	119	150	59	91
0.05		-485	134	143	55	92
1.00		-491	98	161	49	93
0		-440	61	86	886	-
0.01		-446	78	93	237	76
0.05	313	-509	115	126	133	85
0.01		-493	85	107	121	86
0.05		-489	88	118	86	90
1.00		-490	86	115	83	91
0		-430	73	115	3622	-
0.01		-438	85	118	1575	57
0.05	333	-457	92	125	748	79
0.01		-465	94	126	660	82
0.05		-471	92	135	482	87
1.00		-476	108	147	381	90
0		-448	94	222	18209	-
0.01		-439	97	234	12959	29
0.05	353	-433	64	126	5498	70
0.01		-432	72	154	5206	71
0.05		-447	98	180	4116	77
1.00		-444	103	168	3655	80

Fig. 7 illustrates the polarization curves of carbon steel in 1 M HCl solution in the absence and presence of different concentrations of extract at different temperatures. The electrochemical parameters include the corrosion potential, cathodic Tafel slope, anodic Tafel slope, the corrosion current density and inhibition efficiency, which are obtained from the Tafel extrapolation and listed in Table 3. From Fig. 7, the corrosion current densities decline remarkably with the presence of corrosion inhibitor. It can be attributed to the adsorption of inhibitor molecules at the active sites of metal surface, which results in retarding the dissolution of metal and hydrogen evolution at the same times [36]. Besides, it is noted that all the polarization curves are similar in shape, which indicates that the extract of *Basella rubra* fruit has similar inhibition mechanism for carbon steel in hydrochloric acid solution [37]. It can be seen in Table 3 that the corrosion current densities decrease and inhibition efficiency increase with the increase of inhibitor concentration. The corrosion potential presents a slight shift to negative value in the presence of inhibitor by comparing with blank solution. It is regarded in literature that the shifting amount of corrosion potential with inhibitor addition is more than 85 mV to blank solution, the inhibitor may be defined as cathodic or anodic inhibitor [17]. Otherwise, it is commonly deemed as mix-typed inhibitor. In our present study, shifting amount of corrosion potential in the presence of extract is less than 85 mV, suggesting that the inhibitor of *Basella rubra* extract act as a mix -typed inhibitor with cathodic predominance. Moreover, it is found that the corrosion current density increases and inhibition efficiency decreases with the rise of temperature in the same concentration of inhibitor. This phenomenon can be explained as that the rise of temperature leads to increase the oxidation rate of carbon steel in corrosive medium [38]. Most importantly, the peak value of inhibition efficiency reaches 79.9 % at extract

concentration of 1 g L^{-1} at 353 K, which suggests that the extract have good inhibition even in high temperature for carbon steel in 1 M HCl solution.

3.2.3 EIS measurements

Both Nyquist plots and Bode plots of carbon steel in 1 M HCl solution in the absence and presence of different concentrations of inhibitor at different temperatures are shown in Fig. 8. It is shown that the shapes of all the impedance spectra are not a perfect semicircle but a depressed semicircle. It is usually owing to frequency dispersion of interfacial impedance, which is resulted from different physical phenomena presented in the metal surface including roughness, inhomogeneous, impurities and distribution of the surface active sites [39]. The capacitive loops illustrated in Fig. 8 imply that there only exists one time constant in this corrosion process, which is controlled by the charge transfer. The shape of semicircle still keeps the same when adding different concentrations of extract corrosion inhibitor, indicating the similar corrosion mechanism in all solutions [31,40]. Besides, the diameter of semicircle is enlarged with the concentration of extract increasing and declined with temperature rising. The plots of log |*Z*| (*Z* is module value) vs *f* (Frequency) and θ (phase angle) vs f are also shown in Fig. 8. Log |*Z*| remarkably increases in the presence of extract than in blank solution at all temperatures. Only one peak of phase angle variation is presented in the plots of θ vs. f. It is further proved that this corrosion process exists only one time constant in all solutions. According to above results, the proper equivalent circuit of EIS results is shown in Fig. 9 (a), in which Rs is the resistance of solution, Rct represents charge transfer resistance, CPE is a constant phase element and L is inductance with a small value to reduce the fit error. The parameters fitted from EIS are summarized in Table 4. On the one hand, the double layer capacitance is obtained by following equation (Eq. (9)) [36,41].

$$C_{\mathrm{dl}} = \frac{1}{2\pi f_{\max} R_{\mathrm{CT}}} \quad (9)$$

where $f_{\max}$ represents the frequency at which the imaginary component of the impedance (-*Z*") reaches maximum. R_{ct} is the charge transfer resistance. On the other hand, the double layer capacitance is expressed by the Helmholtz model (Eq. (10)) [42].

$$C_{\mathrm{dl}} = \frac{\varepsilon \varepsilon_0}{d} A \quad (10)$$

where d is the thickness of the film, ε and ε_0 are the dielectric constant of the medium and vacuum, respectively. A is the effective area of the electrode.

It can be seen from Table 4 that the charge transfer resistance and double layer capacitance decrease prominently with the increase of extract concentration. However, the inhibition efficiency presents the opposite tendency. Additionally, it is noticeable that inhibition efficiency decreases with the elevating of temperature at the same concentration of extract. The decrease of C_{dl} in the presence of corrosion inhibitor is due to the decline of local dielectric constant or the increase of thickness of the capacitor. The phenomenon can be ascribed to the adsorption of inhibitor molecules on metal surface [41]. Maximum inhibition efficiency of 94.3% occurs at extract concentration of 1 g L^{-1} in 293 K. These results further demonstrate that the inhibitor exhibits excellent inhibition performance for carbon steel in HCl solution. Inhibition efficiencies obtained from both weight loss experiments and electrochemical results are in good agreement.

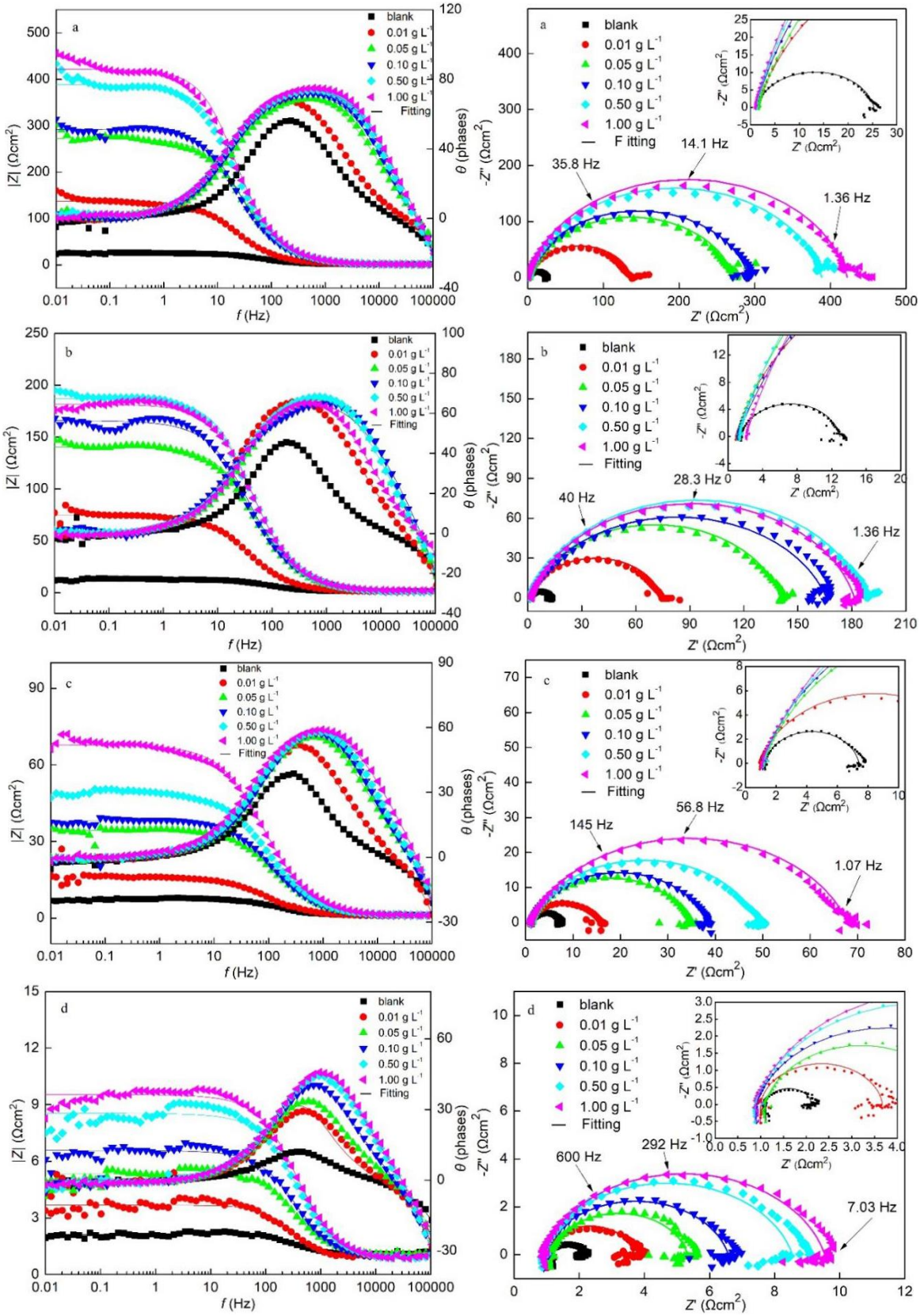

Figure 8. Nyquist and Bode plots for carbon steel in 1 M HCl solution in the absence and presence of different concentrations of extract at temperatures: a) 293 K, b) 313 K, c) 333K, d) 353 K.

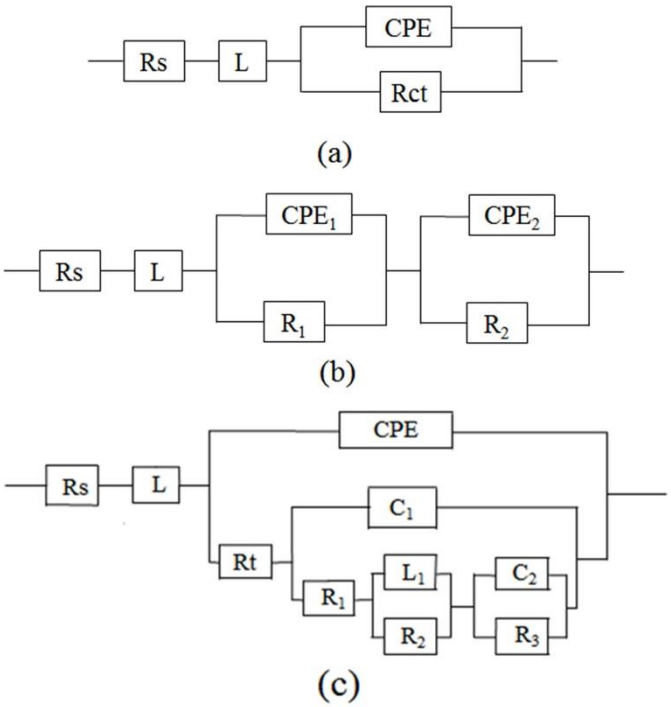

Figure 9. Equivalent circuits used to fit the EIS results: a) for all EIS in Figure8; b) for EIS of carbon steel in HCI after immersed for 64 h; c) for EIS of adding C3.

Table 4. EIS parameters for the corrosion of carbon steel in 1 M HCl in the absence and presence of different concentrations of extract at different temperatures.

C (g L^{-1})	T (K)	Rs (Ω cm^2)	C_{dl} ($\mu F/ cm^2$)	CPE (10^6 s^n Ω^{-1} cm^{-2})	n	L (μHcm^2)	R_{ct} (Ωcm^2)	η (%)
0	293	1.3	148	289	0.89	0.74	24	-
0.01		1.6	83	141	0.88	0.72	135	82
0.05		1.6	33	61	0.86	0.93	271	91
0.01		1.1	30	59	0.87	0.83	291	92
0.05		1.1	29	49	0.88	0.94	387	94
1.00		1.0	27	45	0.88	0.84	421	94
0	313	1.5	193	464	0.89	0.85	12	-
0.01		1.0	97	178	0.87	0.75	74	84
0.05		1.1	51	78	0.85	0.91	139	92
0.01		1.1	43	99	0.81	0.96	165	93
0.05		1.3	30	66	0.85	0.97	186	94
1.00		2.1	31	66	0.85	0.86	179	94
0	333	1.3	283	512	0.90	0.77	6	-
0.01		1.0	149	425	0.84	0.79	15	59
0.05		1.2	67	163	0.83	0.72	33	82
0.01		1.1	60	149	0.84	0.78	37	84
0.05		1.1	46	151	0.82	0.77	48	87
1.00		1.0	42	146	0.80	0.81	67	91
0	353	1.1	541	758	0.95	0.73	1	-
0.01		1.0	256	476	0.93	0.80	3	62
0.05		1.1	162	382	0.87	0.80	4	76
0.01		1.0	121	346	0.85	0.84	6	82
0.05		1.0	89	261	0.84	0.83	8	87
1.00		1.0	63	234	0.84	0.77	9	88

3.3 Influence of immersion time on corrosion inhibition behavior of extract

As an important influential factor, immersion time in corrosion experiment is necessary to be carried out in revealing long-term performance of corrosion inhibitor. Herein, weight loss measurements were conducted to study the effects of immersion time on corrosion of carbon steel in the absence and presence of extract in 1 M HCl at 293 K. The results are displayed in Fig. 10. The corrosion rate decreases with immersion time in all conditions. Longer time of immersion leads to a relatively constant corrosion rate, indicating a stable corrosion event on metal surface has been established. The result can be ascribed to the equilibrium of adsorption-desorption of inhibitor on metal surface to form protective film [19,31]. Fig 10 also presents the relationship between inhibition efficiency and immersion time, the inhibition efficiency keeps stable in the range of studied immersion time. It reveals that the inhibitor can provide persistent protection for carbon steel in HCl solution.

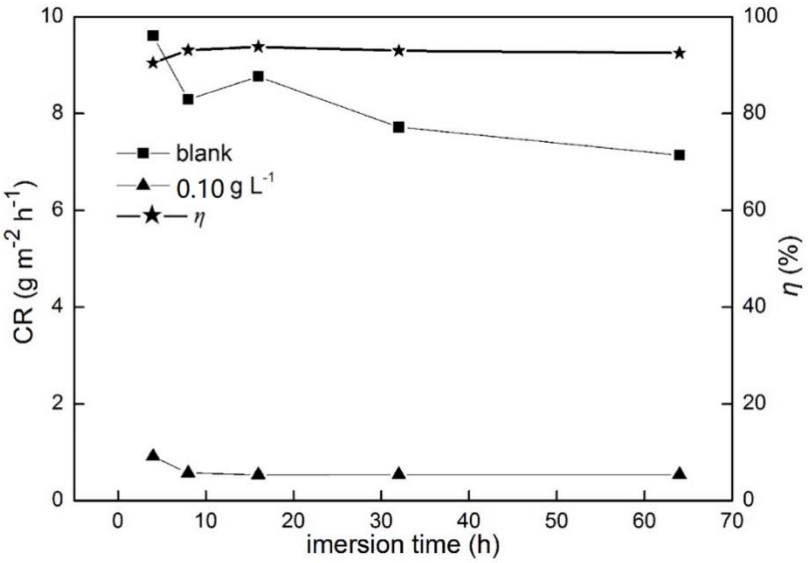

Figure 10. Influence of immersion time on corrosion rate and inhibition efficiency of carbon steel in the absence and presence of 0.10g L^{-1} extract in 1 M HCl at 293 K

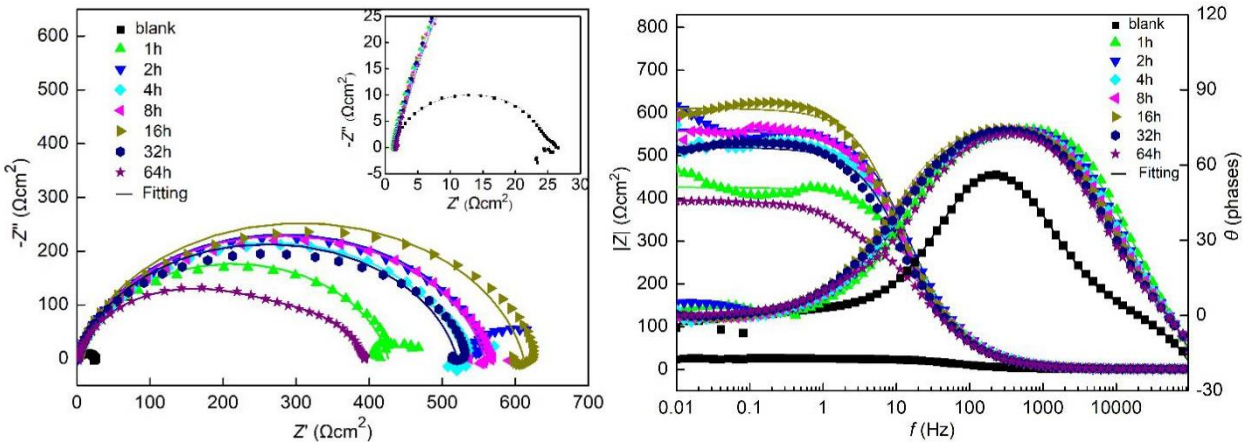

Figure 11. Nyquist and bode plots for carbon steel in 1 M HCl solution in the absence and presence of 0.10 g L^{-1} extract at 293 K in 64 h.

Fig. 11 shows Nyquist plots of carbon steel in 1 M HCl solution in the absence and presence of 0.10 g L^{-1} extract at 293 K in 64 h. It can be seen from Fig. 11 that the diameter of semicircle increases with immersion time from 1 h to 16 h, the largest semicircle occurs at 16 h, which indicates that the adsorption of inhibitor molecules on the metal surface reaches the most compact state at 16 h. With the immersion time further prolonged, the inhibitor film formed on the surface decays slowly [43]. Nyquist plots exhibit one capacitive loop in the studied range from 1 h to 32 h, indicating one time constant in this corrosion process. However, the Nyquist plot presents a slight change at 64 h and two capacitive loops can be observed. The first capacitive loop is controlled by charge transfer, the other one may be attributed to the complicated phenomenon occurred in the interface between metal surface and solution [17,44]. Therefore, based on the above results, Fig. 9 (a) and (b) equivalent circuits are adopted to fit experiment results [45]. Relative EIS parameters are summarized in Table 5.

Table 5. EIS parameters for the corrosion of carbon steel in 1 M HCl in the absence and presence of 0.10 g L^{-1} extract at 293 K

inhibitor	t (h)	R_s (Ω cm^2)	R_{ct} (Ωcm^2)		L ($\mu H cm^2$)	C_{dl} ($\mu F/ cm^2$)	n	
			R_1	R_2			n_1	n_2
blank extract	-	1.3	24		0.74	148	0.89	
	1	1.1	425		0.75	27	0.88	
	2	1.4	560		0.85	25	0.88	
	4	1.4	528		0.85	34	0.87	
	8	1.4	557		0.85	32	0.87	
	16	1.5	610		0.84	37	0.88	
	32	1.5	519		0.83	35	0.87	
	64	1.7	261	131	0.76	-	0.90	0.88

3.4 Constituents of extract as corrosion inhibitors for carbon steel in HCl solution.

Because of a relatively complicated mixture of *Basella rubra* fruit extract, further separation of the extracts can clarify which constituent is more efficient in inhibiting corrosion of carbon steel in HCl solution. Therefore, comparative experiments between extracts and separated constituents had been carried out in this part.

3.4.1 FT-IR results

The FT-IR spectroscopy of extract, C1, C2 and C3 is shown in Fig. 12. A broad peak appears around 3400 cm^{-1} is attributed to O–H or N–H stretching vibration for extract, C2 and C3. A small peak at 2930 cm^{-1} is assigned to C–H stretching vibration for extract, C1 and C3. The peak around 1650 cm^{-1} is related to C=O and C=N stretching vibration, which has been observed in all compounds. The one at 1540 cm^{-1} can be attributed to $–NO_2$ and N–H stretching vibrations. The rest peaks in all compounds can be corresponded to the C–H group of aliphatic and aromatic. The FT-IR results also show that all these compounds (extract, C1, C2 and C3) contain oxygen and nitrogen atoms in functional groups (O–H, N–

H, C=O, C=N etc.) and aromatic ring, which suggests that the compounds are in accordance with the structures of typical corrosion inhibitors [46,47].

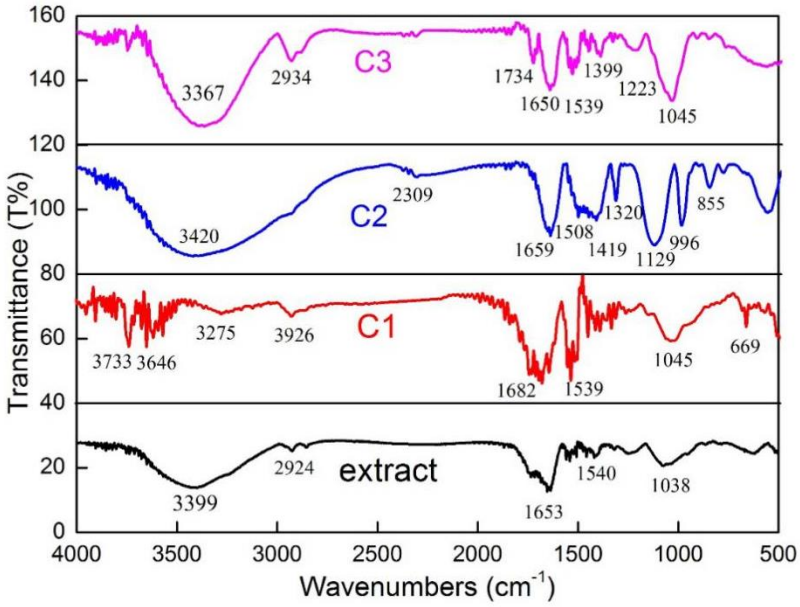

Figure 12. FT-IR results of extract, C1, C2, C3.

3.4.2 Open circuit potential (OCP)

Fig. 13 displays the variations of OCP with time for carbon steel in the absence and presence of 0.10 g L^{-1} different compounds in 1 M HCl solution at 293 K. It is pronounced that the variations of OCP vs. immersion time differ with the addition condition of corrosion inhibitor. In the absence of corrosion inhibitor, OCP shifts to positive direction gradually with the immersion time and then reaches nearly a constant value, indicating a stable corrosion state, in which the corrosion reaction undergoes at a relatively stable rate. The variation of OCP in C2 is close to the absence of corrosion inhibitor, implying similar process. It is also noticed that the OCP of C2 moves positively to a peak and then decreases gradually. This behavior can be attributed to the competition between inhibitor adsorption process and corrosion dissolution process. However, OCPs of extract, C1 and C3 behave differently. It keeps moving negatively and levels off gradually after a long time immersion. The far different performance can be ascribed to the predominance of inhibitor adsorption and film-forming process at interface. Negatively moving of potential also manifests the adsorption of inhibitors influences the cathodic process mainly [15].

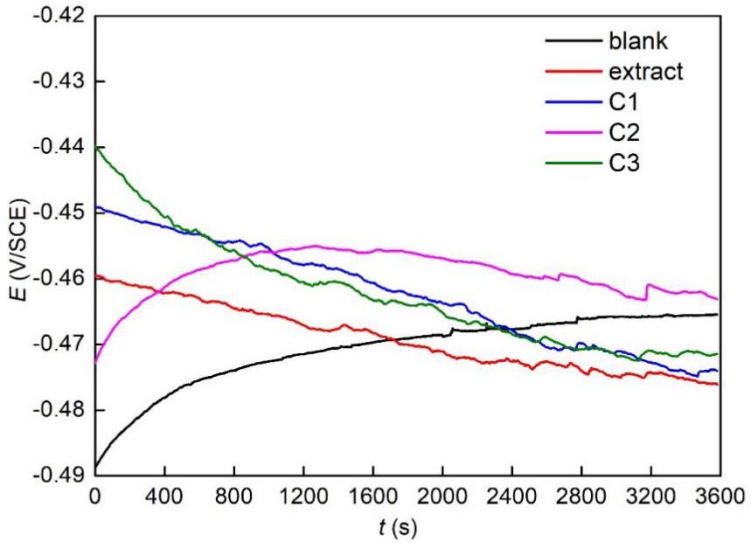

Figure 13. Open circuit potential (OCP) of carbon steel in the absence and presence of 0.10 g L^{-1} different inhibitors in 1 M HCl solution at 293 K.

3.4.3 Potentiodynamic polarization curves

The polarization curves of carbon steel in the absence and presence of 0.10 g L^{-1} different inhibitors in 1 M HCl are shown in Fig. 14. It can be pointed out that these compound inhibitors reduce both cathodic and anodic corrosion current density but cathodic more apparently. Also, the curves of C2, C3 and extract are almost overlapped. The parameters of polarization curves were summarized in Table 6. It can be seen from Table 6 that inhibition efficiency reaches 90% for these compounds except C2. The slight change of corrosion potential indicates that these inhibitors acted as mix-typed inhibitor.

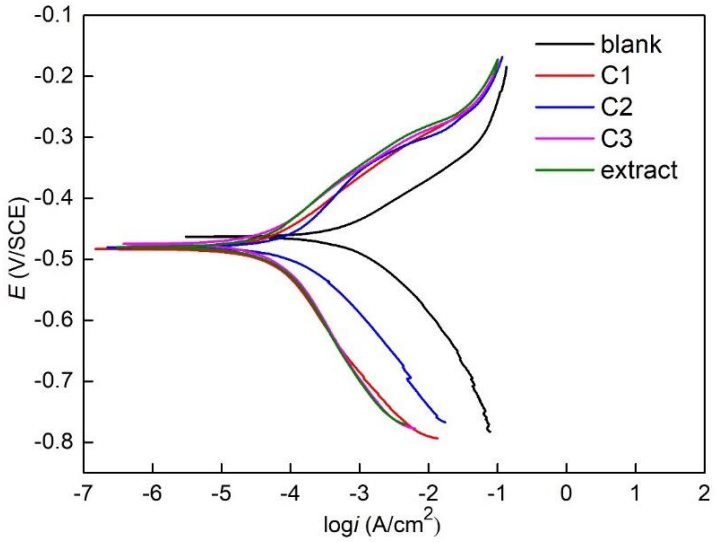

Figure 14. Polarization curves for carbon steel in 1 M HCl solution in the absence and presence of 0.10 g L^{-1} different compounds at 293 K.

Table 6. Parameters fitted from polarization curves of carbon steel in 1 M HCl solution in the absence and presence 0.10 g L^{-1} different corrosion inhibitors at 293 K

inhibitor	E_{corr} (mV)	B_a (mV dec^{-1})	$-B_c$ (mV dec^{-1})	I_{corr} (μA cm^{-2})	η (%)
blank	-463	83	98	647	-
extract	-480	119	150	59	91
C1	-483	100	170	60	91
C2	-480	130	112	113	83
C3	-475	102	157	54	92

3.4.4 EIS measurements

Fig. 15 compares the Nyquist and Bode plots for carbon steel in the absence and presence of 0.10 g L^{-1} different compounds in HCl solution at 293 K. The impedance spectra include a large capacitive loop in the studied range for Compound C1 and Compound C2. However, the impedance spectra of Compound C3 includes a large capacitive loop, a small inductive and a small capacitive in the range of frequency. Hence, the proper equivalent circuits are shown in Fig 9 (a) and (c) to fit experiment data [41,48]. CPE is constant phase element. L is the inductance of a small value to reduce the fit error. Capacitance C1 and Capacitance C2 are double layer capacitance. R_1, R_2 and R_3 are resistances which accord with the large capacitive loop at high frequency, the inductive loop at middle frequency and the small capacitive loop at low frequency, respectively. For equivalent circuit of Fig 9 (c), the polarization resistance R_p is obtained by following equation (Eq. (11)) [48] :

$$R_p = R_t + R_1 + R_2 + R_3 \quad (11)$$

EIS parameters are presented in Table 7. It can be seen that the inhibition efficiency reaches 90% in the presence of different compounds. The result indicates that these compounds can effectively adsorb on the metal surface to inhibit the corrosion of metal. The results of polarization curves and EIS of C1, C2, C3 and extract are in good agreement.

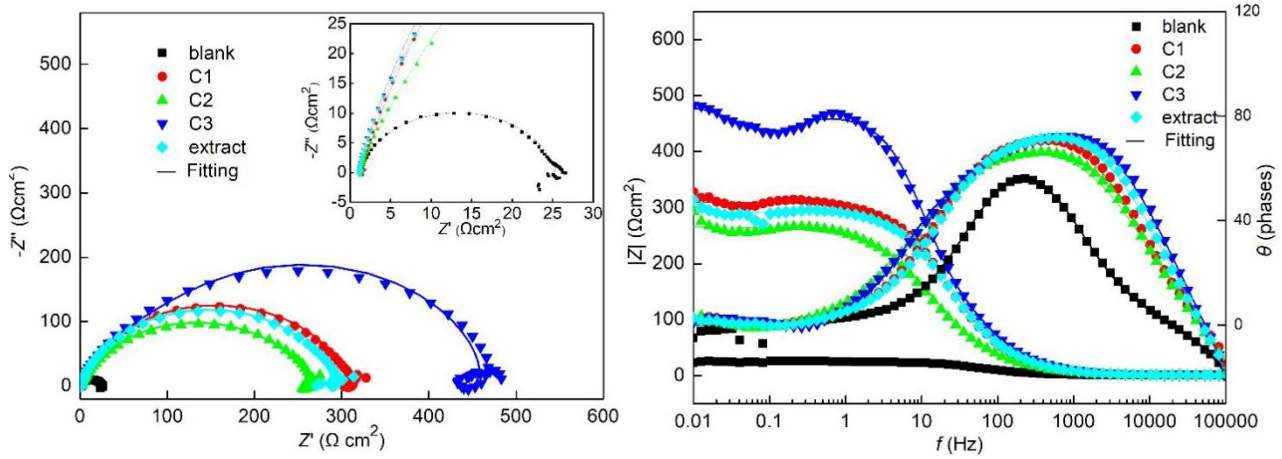

Figure 15. Nyquist and Bode plots for carbon steel in 1 M HCl solution without and with 0.10 g L^{-1} different compounds at 293 K.

Table 7. EIS parameters for the corrosion of carbon steel in 1 M HCl without and with 0.10 g L^{-1} different compounds at 293 K

Inhibitor	R_s (Ω cm^2)	L (μH cm^2)		R_{ct}/R_p (Ω cm^2)	C_{dl} (μF/cm^2)	n	η (%)
		L	L_1				
blank	1.3	0.74	-	24	148	0.89	-
C1	1.4	0.79	-	308	37	0.87	92
C2	1.2	0.82	-	264	68	0.82	91
C3	1.1	0.87	38	529	34	0.89	96
extract	1.1	0.74	-	291	30	0.87	92

3.5 Surface morphologies and inhibition mechanism of inhibitor.

3.5.1 Scanning electron microscopy (SEM)

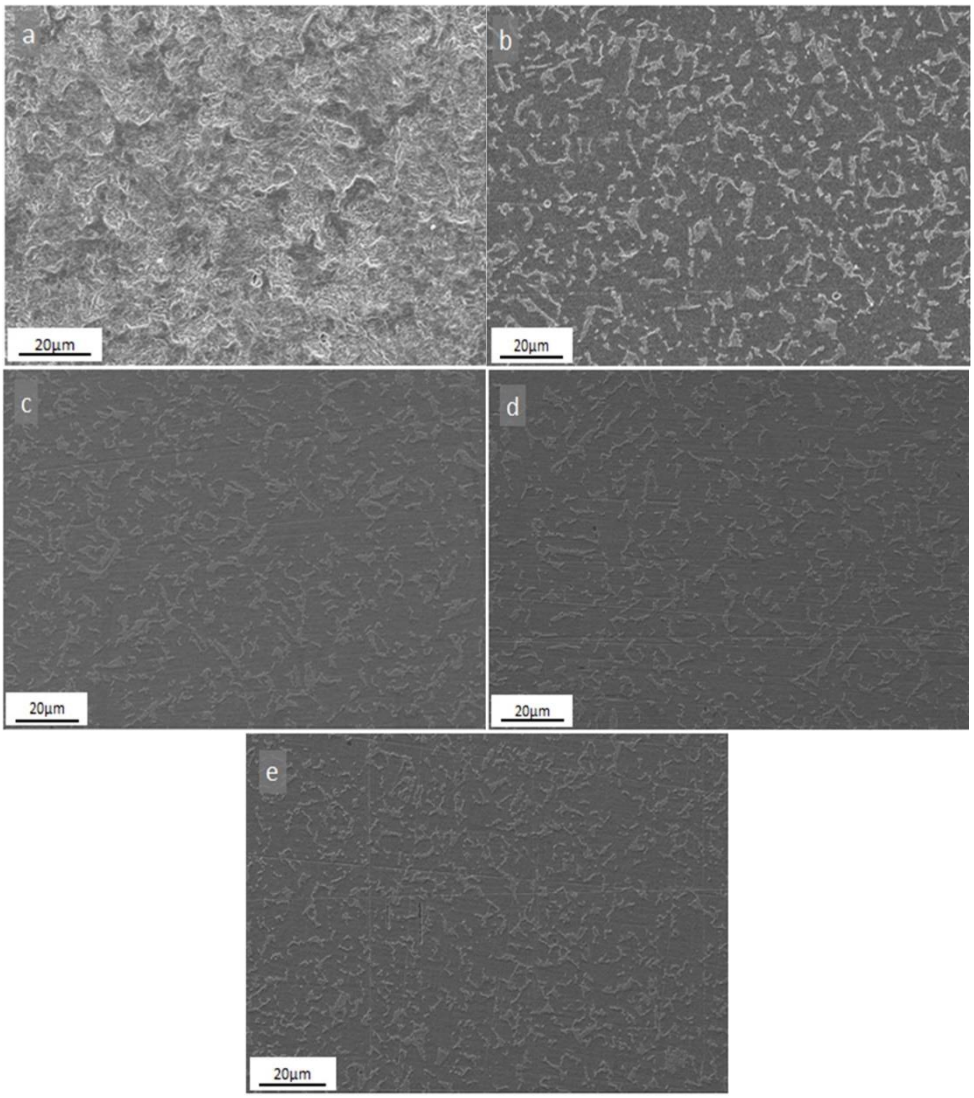

Figure 16. SEM morphologies of carbon steel immersed in 1 M HCl without a) and with 1.00 g L^{-1} extract b), C1 c), C2 d), C3 e) at 293 K.

Fig. 16 shows the SEM morphologies of carbon steel after immersing 4 hours in 1 M HCl in the absence and presence of 1.00 g L^{-1} *Basella rubra* extract at 293 K. It can be seen from Fig. 16 (a) that the surface of carbon steel appears seriously attacked after immersion in solution without inhibitor. It also appears that it is mainly uniform corrosion. By comparing with Fig. 16 (a), it is obviously that the corrosion has been more or less inhibited in the presence of any of the corrosion inhibitors. It is due to the adsorption of inhibitor molecules on the steel surface to form a protective film and then isolate the metal from corrosion medium. Therefore, it can be concluded that the *Basella rubra* extract as well as C1, C2 and C3 can efficiently reduce the corrosion of carbon steel in HCl solution.

3.5.2 X-ray photoelectron spectroscopy (XPS) analysis

In order to confirm the chemical composition of adsorption film and elucidate the adsorption mechanism of the *Basella rubra* extract. XPS measurement was carried out to analysis the surface of carbon steel after immersion in different corrosion inhibitors. Fig. 17 shows XPS of C 1s, O 1s, Fe 2p for carbon steel after immersion for 4h in 1M HCl solution with 1.00 g L^{-1} of extract, C1, C2 and C3. The C 1s spectra for extract, C1 and C2 exhibit three peaks. It is noticed that the C 1s of extract and C1 display three peaks at a binding energy 284.8 eV, 285 eV and 288.6 eV. The peaks at binding energy 284.8 eV and 285 eV can be attributed to the C-C, C=C and C-H aromatic bonds. Another peak at binding energy 288.6 eV is owed to COO and C=O bonds. The XPS peaks for C2 at binding energy 285 eV, 286.5 eV and 288.9 eV can be ascribed to C-C, COO and C=O bonds of the inhibitor molecules. In comparison to extract, C1, and C2, the C 1s spectra of C3 was deconvoluted into four peaks at binding energy 285 eV, 286.5 eV, 288.5 eV and 289.7 eV which are mainly due to the adsorbed organic groups C-C, C=C ,C-H ,COO and C=O [17,49,50].

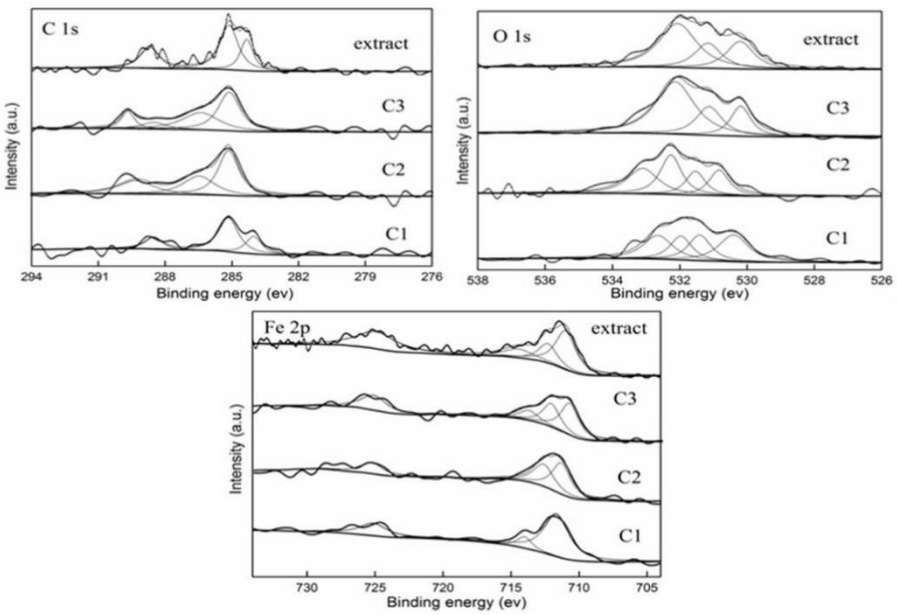

Figure 17. The XPS deconvoluted profiles of C 1s, O 1s, Fe 2p for carbon steel after immersion for 4h in 1M HCl solution with 1.00 g L^{-1} of extract, C1, C2 and C3, respectively.

The O 1s spectrum for extract and C3 could be fitted into three peaks. The first peak, the binding energy at 530.1 eV, is attributed to O^{2-} and bonded to Fe^{3+} in the Fe_3O_4 and /or Fe_2O_3 oxides. The second peak at 531.7 eV can be assigned to OH^- which can be easily to combine with FeO formed hydrous iron oxides (FeOOH) [17]. The third peak at 532 eV is ascribed to O-C-O bond [50]. For C1 and C2, the O 1s spectrum can be fitted into four peaks. These peaks at 530.1 eV, 531.7 eV and 532 eV are the same as extract spectrum peaks. The rest of peak at 532.9 eV can be assigned to C-O bond [49].

The Fe 2p XPS spectra for extract and C3 adsorbed film peaks at binding energy 711 eV, 712.5 eV, 713.6 eV and 724.3 eV, owing to presence of FeO, Fe2O3, FeCl3 and FeOOH. It is noticed that the Fe 2p XPS spectra for C1 and C2 are contained three peaks at around 711 eV, 713.6 eV, 724.3 eV and 711 eV, 712.5 eV, 724.3 eV, respectively. The peaks for binding energy at 711 eV and 724.3 eV are attributed to Fe3+ compound and FeOOH. The binding energy at 713.6 eV is attributed to $FeCl_3$ on the carbon steel surface which may be result from the test environment [49,51]. The iron oxide/hydroxide films (such as Fe_2O_3 and FeOOH) can retard ionic diffusion and increase the corrosion resistance of carbon steel in the corrosion medium. The XPS results demonstrate adsorption of extract, C1, C2 and C3 on carbon steel surface.

3.5.3 Inhibition mechanism of inhibitor

It was reported that the *Basella rubra* fruit mainly include betanin, isobetanin and gomphrenin I [20]. These compounds as major pigments component exist in *Basella rubra*. Therefore, these compounds are easily to adsorb on the metal surface to isolate the corrosive medium. FT-IR results revealed that the extract as well as C1, C2 and C3 contained oxygen and nitrogen atoms in functional groups (O–H, N–H, C=O, C=N etc.) and aromatic ring, which suggest that these compounds are in accordance with the structures of typical corrosion inhibitors [46,47]. The *Basella rubra* inhibitor inhibits the corrosion of carbon steel in hydrochloric acid solution, owing to adsorption of effective components on the steel surface. This conclusion can be drawn from SEM and XPS results which indicated that the inhibitor molecules presented in the surface of carbon steel. Considering the above results, the inhibition mechanism of extract on carbon steel in HCl solution can be ascribed to the forming of complex protective layer via a strong physisorption and chemisorption between extract and carbon steel surface.

4. CONCLUSIONS

(1) The extract of *Basella Rubra* fruit exhibits excellent inhibition efficiency for carbon steel in 1 M HCl. It increases with the concentration of extract and decreases with the temperatures. Maximum inhibition efficiency of 94.8% is achieved with extract concentration of 1.00 g L^{-1} at 293 K.

(2) The adsorption process belongs to mixed type adsorption (both physisorption and chemisorption). Adsorption of the extract obeys Langmuir adsorption isotherm.

(3) Potentiodynamic polarization curves results show that the extract acts as mix-typed inhibitor with cathodically predominant. EIS reveals that the charge transfer resistance increases with the concentration of extract, decreases with the temperatures.

(4) Constituents from extract, C1, C2 and C3, also exhibit excellent inhibition efficiency. C3 is the best constituent in all.

(5) Surface morphologies (SEM) of carbon steel after weigh loss experiments prove all the extract corrosion inhibitors are highly effective in inhibiting corrosion process. XPS analysis demonstrates that the composition of protective layer contained extract molecules, iron oxides and chloride.

ACKNOWLEDGEMENT
This work was supported by the National Key Research and Development Program of China under Grant 2017YFF0204703. We acknowledge its support and funding for this research.

References

1. G. Ji, S. Anjum, S. Sundaram and R. Prakash, *Corros. Sci.*, 90 (2015) 107.
2. C.M. Fernandes, L.X. Alvarez, N.E. Santos, A.C.M. Barrios and E.A. Ponzio, *Corros. Sci.*, 149 (2019) 185.
3. C.M. Fernandes, T.S.F. Fagundes, N.E. Santos, T. M. Rocha, R. Garrett, R.M. Borges, G.Muricy, A.L. Valverde and E.A. Ponzio, *Electrochim. Acta*, 312 (2019) 137.
4. H. Bentrah, Y. Rahali and A. Chala, *Corros. Sci.*, 82 (2014) 426.
5. X.H. Luo, C.G. Ci, J. Li, K.D. Lin, S. Du, H.X. Zhang, X.B. Li, Y.F. Cheng, J.C. Zang and Y.L. Liu, *Corros. Sci.*, 151 (2019) 132.
6. J. Ryl, J. Wysocka, M. Cieslik, H, Gerengi, T. Ossowski, S. Krakowiak and P. Niedzialkowski, *Electrochim. Acta*, 304(2019) 263.
7. G. Moretti, F. Guidi and F. Fabris, *Corros. Sci.*, 76 (2013) 206.
8. I.B. Obot, I.B. Onyeachu and S.A. Umoren, *Corros. Sci.*, 159 (2019) 108140.
9. M.A. Quraishi, A. Singh, V. Kumar, D. Kumar and A. Kumar, *Mater. Chem. Phys.*, 122 (2010) 114.
10. D.E. Abd-El-Khalek, B.A. Abd-El-Nabey and A.M. Abdel-Gaber, *Port. Electrochim. Acta*, 30 (2012) 247.
11. C.D.Taylor, S. Li and A.J. Samin, *Electrochim. Acta*, 269 (2018) 93.
12. P. Mourya, S. Banerjee and M.M. Singh, *Corros. Sci.*, 85 (2014) 352.
13. A. Ostovari, S.M. Hoseinieh, M. Peikari, S.R. Shadizadeh and S.J. Hashemi, *Corros. Sci.*, 51 (2009) 1935.
14. N.A. Odewunmi, S.A. Umoren and Z.M. Gasem, *J. Ind. Eng. Chem.*, 21 (2015) 239.
15. M. Nouha, D. Veys-renaux, E. Rocca and I. Ioannou, *Corros. Sci.*, 102 (2016) 55.
16. C. De Tecnologia, R. De Janeiro and C. De Tecnologia, *Mater. Res.*, 17 (2014) 1581.
17. N. El, R. Fdil, M. Tourabi, C. Jama and F. Bentiss, *Appl. Surf. Sci.*, 357 (2015) 1294.
18. A.Y. El-Etre, *Appl. Surf. Sci.*, 252 (2006) 8521.
19. J. R. Vimala, P. Priyadharshini and R. H. Prasanthi, *World J. Pharm. Pharm. Sci.*, 3 (2016) 1704.
20. S. Sravan, P. Manoj and P. Giridhar, *J. Funct. Foods*, 15 (2015) 509.
21. D. Strack, T. Vogt and W. Schliemann, *Phytochemistry*, 62 (2003) 247.
22. K. Rose, B. Kim, K. Rajagopal, S. Arumugam and K. Devarayan, *J. Mol. Liq.*, 214 (2016) 111.
23. Y. Tang, F. Zhang, S. Hu, Z. Cao, Z. Wu and W. Jing, *Corros. Sci.*, 74 (2013) 271.

24. M. Faustin, A. Maciuk, P. Salvin, C. Roos and M. Lebrini, *Corros. Sci.*, 92 (2015) 287.
25. M.V. Fiori-bimbi, P.E. Alvarez, H. Vaca and C.A. Gervasi, *Corros. Sci.*, 92 (2015) 192.
26. M.A. Amin, M.A. Ahmed, H.A. Arida, T. Arslan, M. Saracoglu and F. Kandemirli, *Corros. Sci.*, 53 (2011) 540.
27. X. Wang, H. Yang and F. Wang, *Corros. Sci.*, 52 (2010) 1268.
28. A.K. Singh and M.A. Quraishi, *Corros. Sci.*, 52 (2010) 1529.
29. A.K. Singh and M.A. Quraishi, *Corros. Sci.*, 52 (2010) 152.
30. N. Soltani, M. Behpour, S.M. Ghoreishi and H. Naeimi, *Corros. Sci.*, 52 (2010) 1351.
31. X. Li, S. Deng and H. Fu, *Corros. Sci.*, 62 (2012) 163.
32. Reşit Yıldız, *Corros. Sci*., 90 (2015) 544.
33. K.R. Ansari, M.A. Quraishi and A. Singh, *Corros. Sci.*, 79 (2014) 5.
34. S.S. Abdel, O.A. Hazzazi, M.A. Amin and K.F. Khaled, *Corros. Sci.*, 50 (2008) 2258.
35. G. Xia, X. Jiang, L. Zhou, Y. Liao, H. Wang and Q. Pu, *Corros. Sci.*, 94 (2015) 224.
36. S. Santana, D.A. Araújo, M. Macedo, T. López, M. Magalhães, T. Gadiole, D. Cristina, L. Ferreira, D. Senna and E.D. Elia, *Corros. Sci.*, 65 (2012) 360.
37. Y. Qiang, S. Zhang, L. Guo, X. Zheng, B. Xiang and S. Chen, *Corros. Sci.*, 119 (2017) 68.
38. M. Jokar, T.S. Farahani and B. Ramezanzadeh, *J. Taiwan Inst. Chem. Eng.*, 63(2016) 1876.
39. M. Behpour, S.M. Ghoreishi, N. Mohammadi, N. Soltani and M. Salavati-niasari, *Corros. Sci.*, 52 (2010) 4046.
40. L. Li, X. Zhang, J. Lei, J. He, S. Zhang and F. Pan, *Corros. Sci.*, 63 (2012) 82.
41. K. Zhang, B. Xu, W. Yang, X. Yin, Y. Liu and Y. Chen, *Corros. Sci.*, 90 (2015) 284.
42. M. Farsak, H. Keles and M. Keles, *Corros. Sci.*, 98 (2015) 223.
43. X. Ma, X. Jiang, S. Xia, M. Shan, X. Li and L. Yu, *Appl. Surf. Sci.*, 371 (2016) 248.
44. R.S. Erami, M.Amirnasr, S. Meghdadi, M. Talebian, H. Farrokhpour and K. Raeissi, *Corros. Sci.*, 151 (2019) 190.
45. M. Gojic, *Corros. Sci.*, 43 (2001) 919.
46. S. Deng and X. Li, *Corros. Sci.*, 55 (2012) 407.
47. S.Q. Chen and D. Zhang, *Corros. Sci.*, 136 (2018) 275.
48. X. Li and S. Deng, *Corros. Sci.*, 65 (2012) 299.
49. M. Chevalier, F. Robert, N. Amusant, M. Traisnel, C. Roos and M. Lebrini, *Electrochim. Acta*, 131 (2014) 96.
50. S. Garai, S. Garai, P. Jaisankar, J.K. Singh and A. Elango, *Corros. Sci.*, 60 (2012) 193.
51. S.Y. Cao, D. Liu, H. Ding, J.H. Wang, H. Lu and J.Z. Gui, *Corros. Sci.*, 153 (2019) 301.